Detecting Tubular Structures Via Direct Vector Field Singularity Characterization

Aytekin D. ÇABUK, Erdenay ALPAY and Burak ACAR

Abstract— The initial step of vessel segmentation in 3D is the detection of vessel centerlines. The proposed methods in literature are either dependent on vessel radius and/or have low response at vessel bifurcations. In this paper we propose a 3D tubular structure detection method that removes these two drawbacks. The proposed method exploits the observations on the eigenvalues of the Hessian matrix as is done in literature, yet it employs a direct 3D vector field singularity characterization. The Gradient Vector Flow vector field is used and the eigenvalues of its Jacobian are exploited in computing a parameter free vesselness map. Results on phantom and real patient data exhibit robustness to scale, high response at vessel bifurcations, and good noise/non-vessel structure suppression.

I. INTRODUCTION

Segmentation of tubular structures, such as vessels, bronchi, etc., is an important component of medical image analysis. It is widely used in medical diagnosis of vessel stenosis, inflammation of vasculature and any defects in vessel shape and structure. Segmentation of tubular structures is composed of two major components: Centerline detection and surface segmentation. Although there are methods that address these two components jointly, the general approach is to use the detected centerlines as the apriori information about the tubular structure locations. Consequently, the correct centerline detection is the prerequisite for correct segmentation of tubular structures.

A significant portion of the methods proposed in the literature for centerline detection, relies on the observation that the orthogonal cross sections of tubular structures in 3D exhibit a 2D symmetric/asymmetric Gaussian profile while the 1D profile orthogonal to this cross section is approximately constant. This corresponds to having negative 1D second derivatives on the centerline, along the directions perpendicular to it, and vanishing derivatives along the centerline. As the eigenvalues of the Hessian of a 3D scalar function, which is a symmetric 3×3 real matrix, corresponds to the 1D second derivatives along the corresponding eigenvectors, several measures derived from these eigenvalues have been proposed. The general pattern of eigenvalues of the Hessian is $\lambda_3 \approx \lambda_2 << \lambda_1 \approx 0$.

Lorenz et al. defined *line-structureness* in terms of the ratios of eigenvalues of the Hessian computed at the estimated scale [1]. Sato et al. used the second derivatives

of a set of multiscale Gaussian filters to detect curvilinear structures and to penalize high intensity on vessel walls [2]. Frangi et al., in their widely popular approach, proposed a *vesselness* measure to detect tubular structures by using the eigenvalus of the Hessian [3]. They classified the local structure according to the eigenvalue patterns and defined their vesselness measure in terms of three exponential functions of eigenvalues, to discriminate background, blob-like, plate-like and line-like structures. Krissian et al. presented another multiscale approach based on the eigensystem of the Hessian to extract vessels and directly estimated the radius of the tubular structures [4]. All of these methods suffer from scale dependence, hence requires a multi-scale approach or scale estimation procedures as well as sensitivity parameters that need to be set carefully. To remove the scale dependence, Bauer and Bischof used the Jacobian of a vector field instead of the Hessian where the vector field is computed by using the Gradient Vector Flow (GVF) [5] algorithm [6].

Methods other than Hessian based approaches have also been proposed. Aylward and Bullitt extracted an intensity ridge map representing the vessel medial axis [7]. Zana and Klein used morphology operators to extract bright regions including the vessels and exploited their differential shape characteristics to identify the vessels [8]. Qian et al. proposed to use local pixel intensity distributions to detect vessels [9]. They observed characteristic intensity distributions on circles (for 2D) centered at vessel centerlines. Li and Yezzi represented a 3D curve in 4D by including the vessel width and formulated the vessel detection and segmentation problem jointly as a variational minimization problem in 4D [10]. However, these approaches have not yet gained wide popularity partly due to computational costs and partly due to the intuition and power that the Hessian based methods provide.

In this work, we adopted the use of the GVF vector field to represent the structures in $I(\mathbf{r})$, which provides scale independence, but defined our vesselness measure based on direct 3D vector field singularity characterization using a fractional anisotropy based on measure together with the vector field divergence. The method is comparatively tested on phantom and real patient datasets. The proposed approach is parameter free and has stronger response at vessel bifurcations.

II. METHOD

A. *Bauer and Bischof's Method*

Bauer and Bischof proposed a method to remove the scale dependence of Hessian based approaches while preserving the rest of the theory of Frangi et al. intact [6]. Observing

that the Hessian of a scalar function, $I(\mathbf{r})$, is the Jacobian of ∇I, ie. the gradient vector field, they proposed to build a vector field, $\mathbf{v}(\mathbf{r})$ that coincides with ∇I near vessel centers and use the Jacobian of $\mathbf{v}(\mathbf{r})$ instead of the Hessian of $I(\mathbf{r})$. More specifically, they used the Gradient Vector Flow (GVF) [5], computed using an edgemap of $I(\mathbf{r})$, as $\mathbf{v}(\mathbf{r})$. The conventional methods to calculate the Hessian of an image require multiscale Gaussian filter convolutions, so scale problem arises while detecting tubular structures. Since the Gradient Vector Flow (GVF) computation relies on an edgemap only, it circumvents the scale dependence problem of Hessian based approaches. The GVF vector field is almost curl-free near vessel centers and thus its Jacobian has real eigenvalues that approximate the eigenvalues of the Hessian of $I(\mathbf{r})$.

Bauer et al. applied the vesselness measure defined in [3] and showed good performance on phantom data near vessel centers. However *i)* their method requires an approximate detection of structures, as the GVF vector field is known to be approximately curl-free in the vicinity of structures, but not in general, thus its Jacobian is not guaranteed to have real eigenvalues in general, unlike the Hessian of $I(\mathbf{r})$, *ii)* the vesselness measure employed requires sensitivity parameters to be set for effective performance, *iii)* it has weak response at vessel bifurcation points (as also in [3]).

B. The Proposed Method

The proposed method is based on a robust and parameter free characterization of the singularities of the computed GVF vector, using the eigenvalues of the Jacobian of the GVF vector field which was recently proposed to be used with Frangi et al.'s *vesselness* measure [3], [6]. It relies on masking with discriminant maps to identify the reliable GVF vector field regions, followed by joint singularity detection and symmetry analysis via the divergence maps and a modified version of *the fractional anisotropy* adopted from the DT-MRI literature.

Let $\mathbf{v}(x, y, z) = [v_1(x, y, z) \ v_2(x, y, z) \ v_3(x, y, z)]^T$ be the 3D GVF vector field computed as described in [5]. Then,

$$\mathbf{J_v} = \begin{bmatrix} \partial_x v_1 & \partial_x v_2 & \partial_x v_3 \\ \partial_y v_1 & \partial_y v_2 & \partial_y v_3 \\ \partial_z v_1 & \partial_z v_2 & \partial_z v_3 \end{bmatrix} \quad (1)$$

$$= [\mathbf{e}_1 \ \mathbf{e}_2 \ \mathbf{e}_3] \begin{bmatrix} \lambda_1 & 0 & 0 \\ 0 & \lambda_2 & 0 \\ 0 & 0 & \lambda_3 \end{bmatrix} [\mathbf{e}_1 \ \mathbf{e}_2 \ \mathbf{e}_3]^T \quad (2)$$

where eigenvalues, $\lambda_1 > \lambda_2 > \lambda_3$'s, are the roots of the characteristic equation. The initial masking filter selects the points where the discriminant of the characteristic equation is non-negative which guarantees that $\lambda_i \in \Re$ for $i = 1, 2, 3$. The proposed vesselness measure, ψ, uses the divergence map and the fractional anisotropy as follows:

$$F = \sqrt{\frac{(\lambda_1 - \lambda_2)^2 + (\lambda_1 - \lambda_3)^2 + (\lambda_2 - \lambda_3)^2}{\lambda_1^2 + \lambda_2^2 + \lambda_3^2}} \in [0, 2]$$

$$(3)$$

$$D = \frac{\nabla \cdot \mathbf{v}}{\max(\nabla \cdot \mathbf{v})} \quad (4)$$

$$\mathbf{f} = [D \ F] \quad (5)$$

$$\psi = \begin{cases} \frac{1}{||\mathbf{f} - [-1 \ 1]||^2} & \lambda_2 \leq 0 \\ 0 & o.w. \end{cases} \quad (6)$$

where D is the divergence map normalized with the maximum absolute divergence in the regions with $\lambda_2 \leq 0$ and F is the modified fractional anisotropy measure ($\in [0, 2]$) which represents the structure of the singularity. $F = 0$ corresponds to a perfectly symmetric point singularity ($\lambda_1 \approx \lambda_2 \approx \lambda_3$), $F = 1$ corresponds to a linear singularity as is expected on the centerlines of the tubular structures ($\lambda_1 \approx \lambda_2 < \lambda_3 \approx 0$) and $F = 2$ corresponds to a sheetlike singularity ($\lambda_1 < \lambda_2 \approx \lambda_3 \approx 0$). D, on the other hand is an indicator of structureness and is expected to be close to -1 near the centerlines of the tubular structures since diffused gradient vectors tend to converge on these singularity points. Hence the vesselness measure, ψ is defined as the inverse of euclidean distance between the feature vector $\mathbf{f}$ and $[-1 \ 1]$.

III. EXPERIMENTS

The experiments were conducted on mathematical phantom data with three different geometries different datasets and a real patient dataset. The $151 \times 151 \times 151$ phantom datasets were generated in MATLAB. All phantom structures are designed to have a Gaussian cross-sectional profile with a peak intensity value of 255 on the centerline and $\sigma = r/3$ where r represents the assigned vessel radius. The value of phantom data is set to 0 in regions outside the vessel. The phantom datasets represent a linear structure with linearly increasing radius $r = [20, 60]$, a linear structure with sinusoidally varying radius with a mean radius of 40 and a T-junction with $r = 40$. The real CT dataset was taken from the training datasets of MICCAI 2007 3D Segmentation in Clinic: A Grand Challenge volumetric image database [11]. Pixel spacing is $0.9375mm$ between axial slices with an inter-slice distance of $1.5mm$. The patient was scanned with a Inversion Recovery Prepped Spoiled Grass sequence on a variety of scanners including GE and Siemens, both 1.5 Tesla. The liver was masked from background by applying a manual segmentation mask on the CT scan.

Figure 1 shows the vesselness maps computed by the scale independent method proposed in [6], the results of the proposed vesselness map and the data itself for both phantom and real patient datasets. Presented results are taken from central axial slice. The pixel values are not scaled. The proposed method has a thinner response than the one proposed in [6], thus can locate the vessel centerlines with higher accuracy. Our maps have lower response outside the vessels as can be seen in Figure 1.b in comparison to Figure 1.a. Its response at vessel bifurcations is stronger as demonstrated in Figure 1.h in comparison to Figure 1.g. The scale independence property of [6] is preserved as shown in Figure 1.e. The real patient experiment, Figure 3, clearly demonstrates the robustness of our method to noise and non-vessel structures.
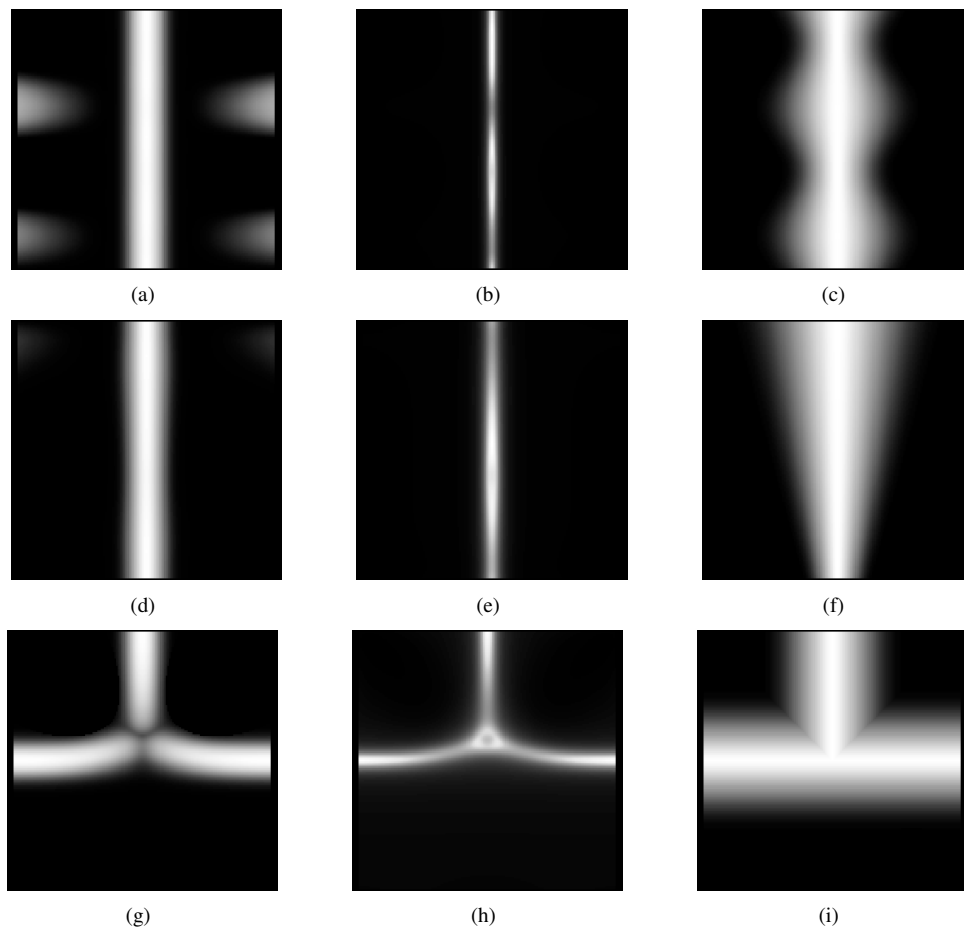
Fig. 1. Comparative results of phantom data experiments. The left column shows the results of the method proposed in [6], the middle column shows our method's results and the right column depicts the geometries of the phantom data and the real data used. The gray scale corresponds to the computed vesselness measure. (a-c) Straight tubular structure with sinusoidally varying radius, (d-f) Straight tubular structure with linearly increasing radius, (g-i) T-junction between two tubular structures.
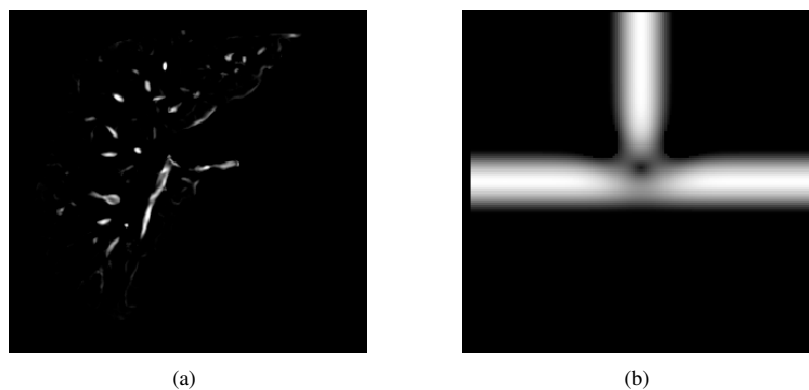

Fig. 2. The vesselness map proposed in [3], applied to (a) the same real patient dataset as in Figure 3.c, (b) the same T-junction phantom dataset as in Figure 1.i.

IV. DISCUSSION AND CONCLUSION

Our method exploits the idea of using a vector field computed by GVF, initially proposed by Bauer and Bischof in [6], which provides scale independence. The response falls off slightly when the diameter of the vessel changes but this is an expected behaviour for most lineness filters [12]. Since the vesselness maps are computed using the GVF vector field, this variation is independent of the vessel radius and is due to the radius variations only. An important property of the proposed method is its higher noise/non-vessel structure suppression in comparison to [6]. This is best demonstrated on the real patient dataset experiment where the previously proposed GVF based method has high response at non-vessel regions that practically masks the vessels. The proposed method also overcomes the weak response of various vesselness measures including Frangi's [3] at bifurcation points. Since bifurcation of vasculature will also be a singularity point of the vector field, our method uses
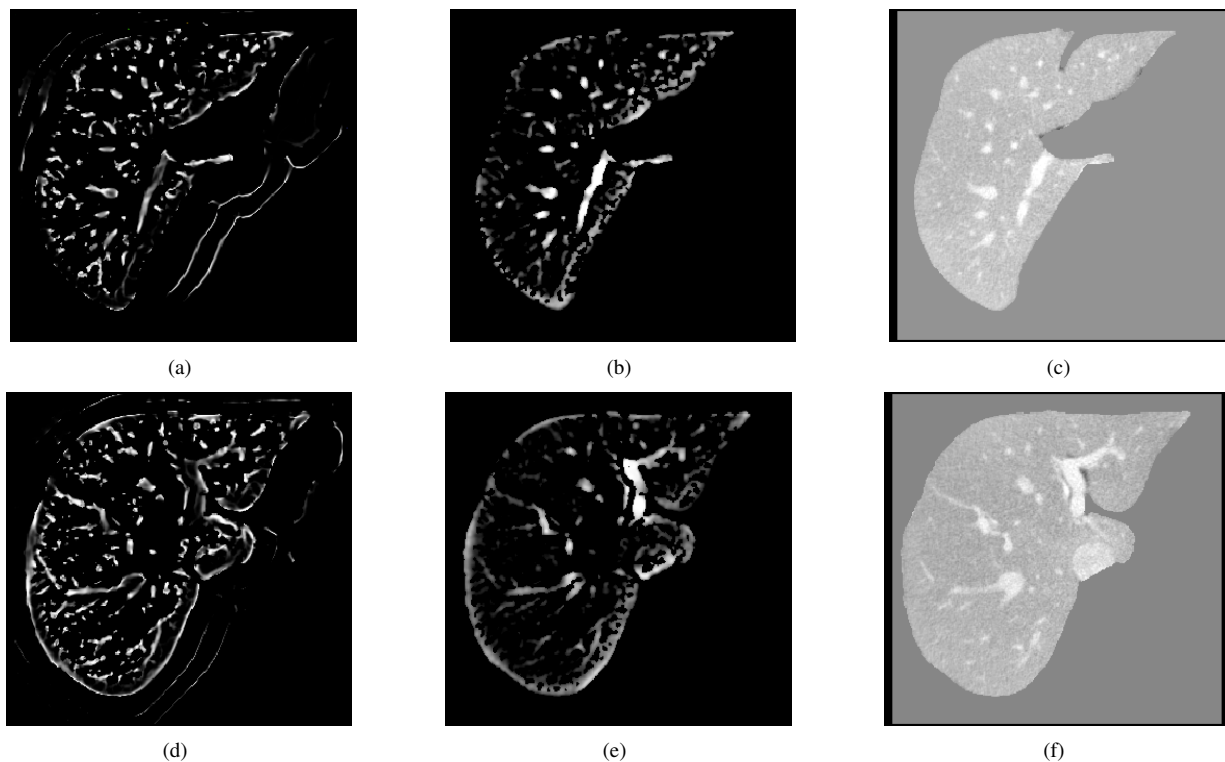
(a)   (b)   (c)

(d)   (e)   (f)

Fig. 3. Comparative results of different slices from the real data experiment. The left column shows the results of the method proposed in [6], the middle column shows our method's results and the right column depicts the real data used. The gray scale corresponds to the computed vesselness measure.

the resultant high divergence (D) to compensate for the low F values (≈ 0.7). Therefore, the feature vector $\mathbf{f}$ turns out to be as close to $[-1 \; 1]$ as non-bifurcating centerline points on vessel centerline. The thinner response of the proposed method provides better centerline localization.

A comparison with the Frangi et al.'s Hessian based method [3] in real patient dataset, as depicted in Figure 2, shows that the proposed method is capable of detecting vessels. We would like to emphasize the scale dependence of the Hessian based approach in computing the partial derivatives of the scalar data and its parameter dependence. The Frangi et al.'s method requires three sensitivity parameters of the exponential functions to be set for proper operation. It also has low response at vessel bifurcations as seen in Figure 2.

As a conclusion, we presented a new method based on vector field singularity analysis that can enhance the response at bifurcation points which is a common problem faced on other tube detection filters. Our method also adresses the size-scale dependency problem that commonly occur in Hessian based approaches, since it results in a thin and pruned response irrespective of size and structure of tubes.

REFERENCES

[1] C. Lorenz, I.-C. Carlsen, T. M. Buzug, C. Fassnacht, and J. Weese, "Multi-scale line segmentation with automatic estimation of width, contrast and tangential direction in 2d and 3d medical images," in *CVRMed-MRCAS'97*, pp. 233–242, Lecture Notes in Computer Science, Springer Berlin / Heidelberg, 1997.

[2] Y. Sato, S. Nakajima, N. Shiraga, H. Atsumi, S. Yoshida, T. Koller, G. Gerig, and R. Kikinis, "Threedimensional multiscale line filter for segmentation and visualization of curvilinear strutures in medical images," *Medical Image Analysis*, vol. 2, no. 2, pp. 143–168, 1998.

[3] A. Frangi, W. Niessen, K. Vincken, and M. Viergever, "Multiscale vessel enhancement filtering," in *Medical Image Computing and Computer-Assisted Intervention-MICCAI'98*, vol. 1496, pp. 130–137, Lecture Notes in Computer Science, Springer Berlin / Heidelberg, 1998.

[4] K. Krissian, G. Malandain, N. Ayache, R. Vaillant, and Y. Trousset, "Model-based detection of tubular structures in 3d images," *Computer Vision and Image Understanding*, vol. 80, no. 2, p. 130, 2000.

[5] C. Xu and J. L. Prince, "Gradient vector flow: A new external force for snakes," *IEEE Computer Society Conference on Computer Vision and Pattern Recognition*, p. 66, 1997.

[6] C. Bauer and H. Bischof, "A novel approach for detection of tubular objects and its application to medical image analysis," in *The 30th DAGM Symposium on Pattern Recognition*, vol. 5096, pp. 163–172, Lecture Notes in Computer Science, Springer Berlin / Heidelberg, 2008.

[7] S. Aylward and E. Bullitt, "Initialization, noise, singularities, and scale in height ridge traversal for tubular object centerline extraction," *IEEE Transactions on Medical Imaging*, vol. 21, no. 2, pp. 61–75, 2002.

[8] F. Zana and J. Klein, "Segmentation of vessel-like patterns using mathematical morphology and curvature evaluation," *IEEE Transactions on Image Processing*, vol. 10, no. 7, p. 1010, 2001.

[9] X. Qian, M. Brennan, D. Dione, W. Dobrucki, M. Jackowski, C. Breuer, A. Sinusas, and X. Papademetris, "A non-parametric vessel detection method for complex vascular structures," *Medical Image Analysis*, vol. 13, no. 1, pp. 49–61, 2009.

[10] H. Li and A. Yezzi, "Vessels as 4-d curves: Global minimal 4-d paths to extract 3-d tubular surfaces and centerlines," *IEEE Transactions on Medical Imaging*, vol. 26, no. 9, pp. 1213–1223, 2007.

[11] T. Heimann, B. V. Ginneken, M. Styner, and et al., "Comparison and evaluation of methods for liver segmentation from ct datasets," *IEEE Transactions on Medical Imaging*, vol. 28, no. 8, pp. 1251–1265, 2009.

[12] H. E. Bennink, H. C. van Assen, G. J. Streekstra, R. ter Wee, J. A. E. Spaan, and B. M. ter Haar Romeny, "A novel 3d multi-scale lineness filter for vessel detection," in *Medical Image Computing and Computer-Assisted Intervention MICCAI 2007*, pp. 436–443, Lecture Notes in Computer Science, Springer Berlin / Heidelberg, 2007.